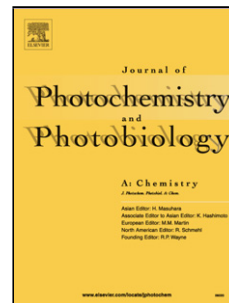


## Accepted Manuscript

Title: Tuning optical absorption in pyran derivatives for DSSC

Author: C. Maglione A. Carella R. Centore S. Fusco A. Velardo A. Peluso D. Colonna A. Di Carlo



PII: S1010-6030(16)00021-6  
DOI: <http://dx.doi.org/doi:10.1016/j.jphotochem.2016.01.018>  
Reference: JPC 10117

To appear in: *Journal of Photochemistry and Photobiology A: Chemistry*

Received date: 27-7-2015  
Revised date: 9-12-2015  
Accepted date: 16-1-2016

Please cite this article as: C.Maglione, A.Carella, R.Centore, S.Fusco, A.Velardo, A.Peluso, D.Colonna, A.Di Carlo, Tuning optical absorption in pyran derivatives for DSSC, *Journal of Photochemistry and Photobiology A: Chemistry* <http://dx.doi.org/10.1016/j.jphotochem.2016.01.018>

This is a PDF file of an unedited manuscript that has been accepted for publication. As a service to our customers we are providing this early version of the manuscript. The manuscript will undergo copyediting, typesetting, and review of the resulting proof before it is published in its final form. Please note that during the production process errors may be discovered which could affect the content, and all legal disclaimers that apply to the journal pertain.

**Tuning optical absorption in pyran derivatives for DSSC**

C. Maglione<sup>a</sup>, A. Carella<sup>a\*</sup> antonio.carella@unina.it, R. Centore<sup>a</sup>, S. Fusco<sup>b</sup>, A. Velardo<sup>b</sup>, A. Peluso<sup>b</sup>, D. Colonna<sup>c</sup>, A. Di Carlo<sup>d</sup>

<sup>a</sup>Department of Chemical Sciences, University of Napoli Federico II, Complesso Universitario Monte Sant'Angelo, Via Cintia, 80126, Napoli, Italy

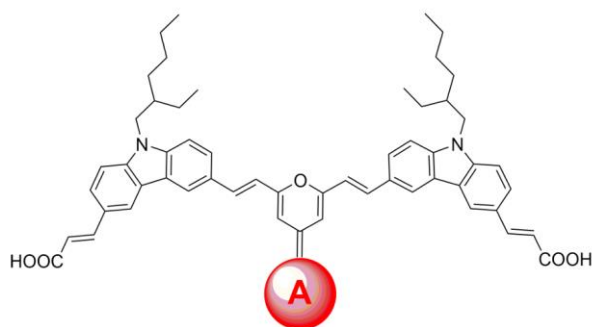
<sup>b</sup>Department of Chemistry and Biology, University of Salerno, via Giovanni Paolo II, Fisciano, I-84084, Italy

<sup>c</sup>DYEPOWER, Viale Castro Pretorio 122, 00185 Roma, Italy

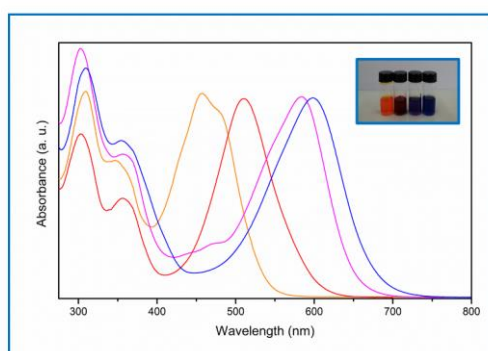
<sup>d</sup>Center for Hybrid and Organic Solar Energy (CHOSE), University of Rome "Tor Vergata", Via Giacomo Peroni 400/402, 00131 Roma

\*Corresponding author.

## Graphical Abstract



Tuning optical absorption along all the visible spectrum



**Highlights**

We synthesized four novel metal free photosensitizers for DSSC

Dyes are based on a pyran acceptor core symmetrically linked to carbazole donor groups

Dyes show colors ranging from orange to blue, covering the most of visible spectrum

The electronic structure of the dyes were investigated at DFT level

DSSC based on the reported chromophores show power conversion efficiency up to 1.9%

**Abstract**

Four novel metal free dyes for application as photosensitizers in DSSC have been synthesized and their chemical-physical properties characterized by Uv-vis absorption spectroscopy, cyclic voltammetry and DFT theoretical computations. The dyes are based on a pyran core, functionalized with different electron acceptor groups, symmetrically linked to carbazole electron donor moieties. The four dyes have different optical absorption properties, affording a range of colors ranging from orange to blue, covering most of the visible spectral region. All the dyes feature high molar extinction coefficient, up to a value of  $1.0 \cdot 10^5 \text{ L} \cdot \text{mol}^{-1} \cdot \text{cm}^{-1}$ . The dyes were used as photosensitizers in DSSC and the photovoltaic characterization of these devices was performed under simulated solar radiation. The cell performance is higher for chromophores featuring higher LUMO energies as a consequence of a better electron injection in  $\text{TiO}_2$  oxide. A maximum power conversion efficiency of 1.9 % has been achieved.

**Keywords:** Synthesis; dyes; pyran; DFT; DSSC.

## 1. Introduction

The intensive exploiting of the fossil fuels reserves, due to the increasing world energy consumption, along with the environmental issues related to the combustion of these energy sources, has fueled in the recent years a growing interest in photovoltaic technology.<sup>1</sup> Solar energy represents the most abundant renewable and clean energy: the coverage of 0.4 % of the world's surface area with photovoltaic modules of 15 % efficiency has been considered sufficient to meet the world's energy needs. While solar energy market is nowadays dominated by silicon, the high production and energy cost of this class of photovoltaics has fostered the development of organic solar cells which could represent a cost-effective viable alternative; moreover, the peculiar mechanical features of organic materials open the way to a range of novel possible applications, not affordable for the rigid and heavy inorganic materials. In this context, dye sensitized solar cells (DSSCs) have attracted considerable attention in the last 20 years<sup>2</sup> and very promising efficiency, up to 11%<sup>3</sup> have been obtained using ruthenium(II)-polypyridyl complexes as photosensitizers. Ruthenium complexes are, anyway, intrinsically expensive and, moreover, feature moderate molar absorption coefficient (around  $20000 \text{ L mol}^{-1} \text{ cm}^{-1}$ ). For these reasons, recent years have seen a growing interest in metal free organic dyes for application in DSSCs, typically constituted by a push-pull molecular structure:<sup>4</sup> the advantages of this kind of system rely on their high molar absorption coefficient and on the tunability of their absorption and electronic properties achievable through a suitable molecular design. Most of synthetic organic dyes used in DSSCs are based on heterocycles.<sup>4a,b</sup> These moieties, in fact, have proven to be very efficient building blocks for the synthesis of active molecules in many fields of advanced materials spanning from liquid crystals<sup>5</sup> and optoelectronics<sup>6</sup> to organic semiconductors<sup>7</sup>. In the field of DSSCs, heterocycles can be used, depending on their character, as electron donor or acceptor groups<sup>4a,b</sup>, as pi-conjugated bridges<sup>4a,b</sup> or even as acidic groups for anchoring to the inorganic semiconductor.<sup>8</sup>

Pyran containing dyes, in particular, represent a class of compounds deeply investigated in the field of organic electronics and photonics; the versatility of the starting building block of this kind of compounds (i. e. 2,6-dimethyl- $\gamma$ -pyrone) has allowed the synthesis of several different molecular structures, affording materials characterized by different interesting properties, such as fluorescence,<sup>9</sup> second order nonlinear

optical activity,<sup>10</sup> two photon absorption,<sup>11</sup> photovoltaic activity.<sup>12</sup> More recently, the use of this class of compounds in DSSCs was investigated.<sup>13</sup>

We report here on novel organic photosensitizers based on an electron acceptor pyran core symmetrically linked, through ethylene bridges, to donor carbazole moieties. Their chemical diagrams are reported in Figure 1.

Carbazole ring is a building block widely investigated in organic electronics, mainly because of its strong electron donor ability and low oxidation potential.<sup>14</sup> Several studies on DSSC photosensitizers containing carbazole moieties in their molecular structure are reported in the literature.<sup>15</sup> In the present work, carbazole groups are functionalized with two acrylic acid moieties for allowing binding to the TiO<sub>2</sub> surface. The enhanced anchoring properties of the dyes due to the presence of two carboxyl groups are expected to increase the binding strength of the photosensitizers to TiO<sub>2</sub>, possibly resulting in an enhancement of charge transfer and cell performance, as shown in previous papers.<sup>16</sup> The pyran core is instead functionalized with electron acceptor groups of different strengths: as also reported in previous works,<sup>17</sup> the functionalization of a same molecular fragment with electron acceptor groups of different strength, is expected to result in the tuning of the optical absorption of the dyes so that different parts of the visible spectrum can be covered.

The synthesized chromophores have been characterized by optical and electrochemical measurements; their electronic structure has been analysed by Density Functional Theory (DFT) and their efficiencies in DSSC tested under simulated sun radiation.

## 2. Materials and methods

### 2.1 Synthesis

All the intermediates used in the synthetic procedures described below, have been purchased by Sigma Aldrich, TCE Europe or Acros Organics, and used without further purification. The only exceptions are 3-

dicianovinylindan-1-one and 2-(1,1-dioxidobenzo[b]thiophen-3(2H)-ylidene)malononitrile (Sandoz group) that have been prepared according, respectively, to references 18 and 19.

***2-(2,6-dimethyl-4H-pyran-4-ylidene)malononitrile (A<sub>1</sub>)***

2,6-dimethyl- $\gamma$ -pyrone (12.50 g, 0.100 mol) and malononitrile (6.90 g, 0.104 mol) were dissolved in 50 mL of acetic anhydride; the solution was refluxed, under nitrogen flux, for 5 h. The system was then slowly cooled down to room temperature and the crystallization of a brown compound occurred. This compound was recovered by suction filtration and recrystallized by chloroform-hexane. Light brown needle-shape crystals were obtained. The yield was 60 %.

<sup>1</sup>H-NMR (CDCl<sub>3</sub>, 200 MHz);  $\delta$ = 2.31 (s, 6H, -CH<sub>3</sub>); 6.53 (s, 2H, pyran CH).

Mp: 192 °C.

***2-(2,6-dimethyl-4H-pyran-4-ylidene)-thiobarbituric acid (A<sub>2</sub>)***

The same synthetic strategy used for the preparation of A<sub>1</sub> was followed; the only difference is that thiobarbituric acid was used instead of malonitrile in the condensation reaction with the pyrone derivative. Yellow needles were recovered after crystallization in CHCl<sub>3</sub>-hexane. The yield was 68 %.

<sup>1</sup>H-NMR (CDCl<sub>3</sub>, 200 MHz);  $\delta$ = 1.30 (t, 6H, J=, -CH<sub>3</sub>); 2.46 (s, 6H, -CH<sub>3</sub>), 4.57 (q, 4H, J=, -CH<sub>2</sub>); 8.82 (s, 2H, pyran CH).

Mp: 195°C.

***2-(2-(2,6-dimethyl-4H-pyran-4-ylidene)-3-oxo-2,3-dihydro-1H-inden-1-ylidene)malononitrile (A<sub>3</sub>)***

The compound was synthesized following the same procedure used for A<sub>1</sub> synthesis, except that 3-dicianovinylindan-1-one was used instead of malononitrile. A brown crystalline solid was obtained after recrystallization (CHCl<sub>3</sub>-hexane). The yield was 58 %.

$^1\text{H-NMR}$  ( $\text{CDCl}_3$ , 400 MHz);  $\delta$ = 2.50 (s, 6H,  $-\text{CH}_3$ ), 7.50 (broad, 1H); 7.60 (m, 3H, Ar-H); 7.74 (d, 1H,  $J=7.0$  Hz); 8.44 (d, 1H,  $J=7.0$  Hz, Ar-H).

Mp: 212 °C

***2-(2-(2,6-dimethyl-4H-pyran-4-ylidene)-1,1-dioxidobenzo[b]thiophen-3(2H)-ylidene)malononitrile (A<sub>4</sub>)***

The compound was synthesized following the same procedure used for A<sub>1</sub> synthesis, except that Sandoz group was used instead of malononitrile. A reddish crystalline solid was obtained. After recrystallization ( $\text{CHCl}_3$ -hexane) The yield was 62 %.

$^1\text{H-NMR}$  ( $\text{CDCl}_3$ , 400 MHz);  $\delta$ = 2.52 (s, 6H,  $-\text{CH}_3$ ), 7.05 (broad, 1H, Ar-H); 7.73 (m, 3H, Ar-H); 8.09 (m, 1H, Ar-H); 8.68 (m, 1H, Ar-H).

Mp: 258 °C

***9-(2-ethylhexyl)-9H-carbazole (1)***

Finely powdered KOH (34.00 g, 0.61 mol) were suspended in DMF (150 mL). The system was kept under stirring at room temperature for 15 min and then, carbazole (16.10 g, 0.0960 mol) was added. After 1 h, 2-ethylhexylbromide (25.28 g, 0.130 mol) was poured in the system and the temperature was raised to 100 °C. After 6 h, the system was cooled down to room temperature and the solid inorganic part filtered off. The filtered solution was poured in 300 mL of water and extracted with hexane (3x100 mL). The organic phase was then washed with brine and water, dried over  $\text{Na}_2\text{SO}_4$  and the solvent removed at reduced pressure. The resulting crude oil was purified by silica gel liquid chromatography (hexane). A colorless oil was recovered. The yield was 75 %.

$^1\text{H-NMR}$  ( $\text{CDCl}_3$ , 400 MHz);  $\delta$ = 0.90 (m, 6H,  $-\text{CH}_3$ ); 1.27-1.40 (m, 8H,  $-\text{CH}_2$ ); 2.07 (broad, 1H,  $-\text{CH}$ ); 4.15 (d, 2H,  $J=8.0$  Hz); 7.23 (t, 2H,  $J=8.0$  Hz, Ar-H); 7.40 (d, 2H,  $J=8.0$  Hz, Ar-H); 7.47 (d, 2H,  $J=8.0$  Hz, Ar-H), 8.11(d, 2H,  $J=8.0$  Hz, Ar-H) .

***3-bromo-9-(2-ethylhexyl)-9H-carbazole (2)***

Compound 1 (23.9 g, 0.0850 mol) was solved in dry DMF; a solution of N-bromosuccinimide (15.22 g, 0.0850 mol) in 25 mL of dry DMF was then poured dropwise in the carbazole solution. The system reacted overnight at room temperature, in the dark. The solution was then poured in 200 mL of water and extracted with diethyl ether (3x100 mL). The organic phase was then washed with brine and water, dried over Na<sub>2</sub>SO<sub>4</sub> and the solvent removed at reduced pressure. The resulting crude oil was purified by silica gel liquid chromatography (hexane/ethyl acetate 80/20 v/v). A yellow oil was recovered. The yield was 75 %.

<sup>1</sup>H-NMR (CDCl<sub>3</sub>, 400 MHz); δ= 0.87 (t, 3H, J=7.2 Hz, -CH<sub>3</sub>); 0.90 (t, 3H, J=7.2 Hz, -CH<sub>3</sub>); 1.24-1.40 (m, 8H, -CH<sub>2</sub>); 2.07 (broad, 1H,-CH); 4.15 (d, 2H, J=8.0 Hz); 7.22 (d, 2H, J=8.0 Hz, Ar-H); 7.37-7.55 (m, 3H, Ar-H); 8.03-8.20 (m, 2H Ar-H).

### ***3-bromo-9-(2-ethylhexyl)-6-formyl-9H-carbazole (3)***

Dry DMF (20.9 mL, 19.73 g, 0.27 mol) was solved in 25 mL of dry 1,2-dichloroethane (DCE) and kept under nitrogen at 0 °C, in an ice water bath. POCl<sub>3</sub> (25.1 mL, 41.4 g, 0.27 mol) was then added dropwise to the system that, after the addition, was warmed to room temperature. Then compound 2 (15.0 g, 0.0420 mol), solved in 20 mL of dry DCE, was added dropwise and the temperature raised to 90 °C. The system was allowed to react at that temperature overnight and, after being cooled down to room temperature, poured in 400 mL of water. The pH was raised to about 5 by adding 5 % wt NaOH water solution. The obtained emulsion was extracted with chloroform (3x250 mL). The organic phase was washed with brine and water, dried over Na<sub>2</sub>SO<sub>4</sub> and the solvent removed at reduced pressure. The resulting crude oil was purified by silica gel liquid chromatography (hexane/ethyl acetate 80/20 v/v). A yellow oil was recovered. The yield was 65 %.

<sup>1</sup>H-NMR (CDCl<sub>3</sub>, 200 MHz); δ= 0.84 (t, 3H, J=7.2 Hz, -CH<sub>3</sub>); 0.91 (t, 3H, J=7.2 Hz, -CH<sub>3</sub>) 1.23-1.38 (m, 8H, -CH<sub>2</sub>); 2.00 (q, 1H,J=6.4 Hz,-CH); 4.18 (d, 2H, J=8.0 Hz); 7.31 (d, 1H,J=8.7 Hz, Ar-H); 7.46 (d, 1H, J=8.4 Hz, Ar-H); 7.60 (dd, 1H, J<sub>1</sub>=2.0 Hz, J<sub>2</sub>=8.4 Hz, Ar-H); 8.03 (dd, 1H, J<sub>1</sub>=1.4 Hz, J<sub>2</sub>=8.0 Hz, Ar-H); 8.26 (d, 1H, J=2.0 Hz, Ar-H); 8.55 (d, 1H, J=1.4 Hz, Ar-H); 10.09 (s, 1H, CHO).

***(E)-3-(9-(2-ethylhexyl)-6-formyl-9H-carbazol-3-yl)acrylic acid (D)***

Compound **3** (2.000 g, 0.0052 mol) and acrylic acid (3.5 ml, 3.68 g, 0.051 mol) were dissolved in 10 mL of dry DMF; the solution was degassed with nitrogen for 15 minutes and then palladium acetate (0.26 mmol, 58.3 mg), tri-*o*-tolylphosphine (0.157 g, 0.52 mmol) and triethylamine (1.8 mL, 1.307 g, 0.013 mol) were added. The system was kept at 100 °C for 24 h, stirred under nitrogen. The reaction mixture was then cooled down to ambient temperature and poured in 50 mL of water. The aqueous layer was extracted with chloroform (3 x 50 mL). The organic phase is washed with brine and water, dried over Na<sub>2</sub>SO<sub>4</sub> and the solvent removed at reduced pressure. The resulting crude oil was purified by silica gel liquid chromatography (chloroform-methanol 98/2 v/v). A yellow oil was recovered that slowly crystallized at ambient temperature. The yield was 52 %.

<sup>1</sup>H-NMR (CDCl<sub>3</sub>, 400 MHz); δ= 0.84 (t, 3H, J=7.2 Hz, -CH<sub>3</sub>); 0.90 (t, 3H, J=7.2 Hz, -CH<sub>3</sub>); 1.25-1.36 (m, 8H, -CH<sub>2</sub>); 2.00 (broad, 1H, -CH); 4.11 (d, 2H, J=7.6 Hz); 6.44 (d, 1H, J=16.0 Hz, CH=CH); 7.35 (d, 1H, J=8.4 Hz, Ar-H); 7.41 (d, 1H, J=8.4 Hz); 7.66 (d, 1H, J=8.0 Hz, Ar-H); 7.91 (d, 1H, J=16.0 Hz, CH=CH), 8.13 (s, 1H); 8.48 (s, 1H); 10.06 (s, 1H).

***(2E,2'E)-3,3'-(((1E,1'E)-(4-(dicyanomethylene)-4H-pyran-2,6-diyl)bis(ethene-2,1-diyl))bis(9-(2-ethylhexyl)-9H-carbazole-6,3-diyl))diacrylic acid (C<sub>1</sub>)***

Compound A<sub>1</sub> (0.151 g, 0.88 mmol) and D (0.730 g, 1.93 mmol), were dissolved in a solution constituted by 9 mL of CH<sub>3</sub>CN and 1 mL of pyridine. The solution, stirred in nitrogen atmosphere, was taken at reflux temperature and then, five drops of piperidine were added. The solution was refluxed overnight and then poured in 50 mL of MeOH. The precipitation of a compound occurred, that was then recovered by filtration and recrystallized by THF-hexane. An amorphous orange solid was obtained. Yield was 62 %.

<sup>1</sup>H-NMR (DMSO, 500 MHz); δ= 0.74 (t, 6H, J=7.0 Hz, -CH<sub>3</sub>); 0.81 (t, 6H, J=7.0 Hz, -CH<sub>3</sub>); 1.10-1.29 (m, 16H, -CH<sub>2</sub>); 1.92 (m, 2H, -CH); 4.19 (d, 4H, J=6.0 Hz); 6.51 (d, 2H, J=15.0 Hz, CH=CH); 6.64 (s, 2H, pyran CH); 7.25 (d,

2H, J=15.0 Hz, CH=CH); 7.54 (m, 4H, Ar-H); 7.74 (d, 2H, J=15.0 Hz, CH=CH); 7.78-7.80 (m, 6H, Ar-H), 8.42 (s, 2H); 8.59 (s, 2H); 12.23 (s broad, 1H).

<sup>13</sup>C-NMR (DMSO, 75 MHz):  $\delta$ =167.9; 158.7; 155.4; 144.8; 142.0; 141.9; 138.2; 127.2; 126.5; 125.8; 122.6; 122.5; 120.7; 120.4; 116.1; 116.0; 115.7; 110.1; 109.8; 105.6; 55.4; 46.8; 30.1; 28.0; 23.7; 22.4; 13.7; 10.6.

T<sub>g</sub>: 192 °C.

MALDI-TOF-MS: Found: 890.46; 'Molecular formula C<sub>58</sub>H<sub>58</sub>N<sub>4</sub>O<sub>5</sub> requires': 890.44.

CHN elemental analysis: Found: C 78.24 H 6.63 N 6.21 %; 'Molecular Formula C<sub>58</sub>H<sub>58</sub>N<sub>4</sub>O<sub>5</sub> requires': C 78.18; H 6.56; N 6.29 %.

***(2E,2'E)-3,3'-(((1E,1'E)-(4-(1,3-diethyl-4,6-dioxo-2-thioxotetrahydropyrimidin-5(2H)-ylidene)-4H-pyran-2,6-diy))bis(ethene-2,1-diy))bis(9-(2-ethylhexyl)-9H-carbazole-6,3-diy))diacrylic acid (C<sub>2</sub>)***

Compound A<sub>2</sub> (0.185 g, 0.60 mmol) and D (0.500 g, 1.32 mmol), were dissolved in a solution constituted by 9 mL of CH<sub>3</sub>CN and 1 mL of pyridine. The solution, stirred in nitrogen atmosphere, was taken at reflux temperature and then, five drops of piperidine were added. The solution was refluxed overnight and then cooled down to room temperature. The precipitation of a compound occurred, that was then recovered by filtration and recrystallized by THF-hexane. An amorphous purple solid was obtained. Yield was 60 %.

<sup>1</sup>H-NMR (DMSO, 500 MHz);  $\delta$ = 0.73 (t, 6H, J=7.0 Hz, -CH<sub>3</sub>); 0.80 (t, 6H, J=7.0 Hz, -CH<sub>3</sub>); 1.14-1.29 (m, 20H, -CH<sub>2</sub> + CH<sub>3</sub> TB ring); 1.88 (m, 2H, -CH); 4.12 (d, 4H, J=6.0 Hz, N-CH<sub>2</sub> carbazole); 4.33 (q, 4H, N-CH<sub>2</sub> TB ring), 6.54 (d, 2H, J=15.0 Hz, CH=CH); 7.24 (d, 2H, J=15.0 Hz, CH=CH); 7.44-7.46 (m, 4H, Ar-H); 7.70-7.73 (m, 4H, Ar-CH); 7.81 (d, 2H, J=15.0 Hz, CH=CH), 7.88 (d, 2H, J=10.0 Hz, Ar-CH); 8.43 (s, 2H, Ar-H); 8.62 (s, 2H, Ar-H); 8.77 (s, 2H, pyran CH).

<sup>13</sup>C-NMR (DMSO, 75 MHz):  $\delta$ = 176.6; 168.5; 161.0; 160.5.3; 155.9; 142.1; 141.9; 138.7; 138.5; 126.6; 122.8; 116.8; 109.9; 109.7; 95.6; 45.4; 30.4; 28.1; 23.9; 22.4; 13.5; 10.5.

MALDI-TOF-MS: Found: 994.52 (deriving from the fragmentation of two methyl groups), 1024.47; 'Molecular formula C<sub>63</sub>H<sub>68</sub>N<sub>4</sub>O<sub>7</sub>S requires': 1024.48.

CHN elemental analysis: Found: C 73.95 H 6.62 N 5.35 %; 'Molecular Formula C<sub>63</sub>H<sub>68</sub>N<sub>4</sub>O<sub>7</sub>S requires': C 73.80; H 6.69; N 5.46 O 10.92; S 3.13 %.

***(2E,2'E)-3,3'-(((1E,1'E)-(4-(1-(dicyanomethylene)-3-oxo-1,3-dihydro-2H-inden-2-ylidene)-4H-pyran-2,6-diyl)bis(ethene-2,1-diyl))bis(9-(2-ethylhexyl)-9H-carbazole-6,3-diyl))diacrylic acid (C<sub>3</sub>)***

Compound A<sub>3</sub> (0.181 g, 0.60 mmol) and D (0.500 g, 1.32 mmol), were dissolved in a solution constituted by 9 mL of CH<sub>3</sub>CN and 1 mL of pyridine. The solution, stirred in nitrogen atmosphere, was taken at reflux temperature and then, five drops of piperidine were added. The solution was refluxed overnight and then cooled down to room temperature. The precipitation of a compound occurred, that was then recovered by filtration and recrystallized by THF-hexane. An amorphous violet solid was obtained. Yield was 64 %.

<sup>1</sup>H-NMR (DMSO, 500 MHz); δ= 0.76 (t, 6H, J=7.5 Hz, -CH<sub>3</sub>); 0.81 (t, 6H, J=7.5 Hz, -CH<sub>3</sub>); 1.15-1.30 (m, 16H, -CH<sub>2</sub>); 2.05 (m, 2H,-CH); 4.04 (d, 4H, J=6.0 Hz, N-CH<sub>2</sub>); 6.53 (d, 2H, J=15.0 Hz, CH=CH); 7.25 (d, 2H, J=15.0 Hz, CH=CH); 7.42 (d, 2H, J=10.0 Hz, Ar-H); 7.47-7.55 (m, 7H, Ar-CH); 7.73 (d, 2H, J=5.5 Hz, Ar-H), 7.76 (s, 2H, pyran CH); 7.86 (s, 2H, pyran CH); 7.89 (d, 2H, J=5.5 Hz, Ar-H); 8.11 (d, 1H, J= 7.0 Hz, Ar- H); 8.40 (s, 2H, Ar-H); 8.49 (s, 2H, Ar-H); 12.20 (s broad, 2H).

MALDI-TOF-MS: Found: 1018.48; 'Molecular formula C<sub>67</sub>H<sub>62</sub>N<sub>4</sub>O<sub>6</sub> requires': 1018.46.

CHN elemental analysis: Found: C 79.11 H 6.19 N 5.44 %; 'Molecular Formula C<sub>67</sub>H<sub>62</sub>N<sub>4</sub>O<sub>6</sub> requires': C 78.95; H 6.13; N 5.50; O 9.42 %.

***(2E,2'E)-3,3'-(((1E,1'E)-(4-(3-(dicyanomethylene)-1,1-dioxidobenzo[b]thiophen-2(3H)-ylidene)-4H-pyran-2,6-diyl)bis(ethene-2,1-diyl))bis(9-(2-ethylhexyl)-9H-carbazole-6,3-diyl))diacrylic acid (C<sub>4</sub>)***

Compound A<sub>4</sub> (0.201 g, 0.60 mmol) and D (0.500 g, 1.32 mmol), were dissolved in a solution constituted by 9 mL of CH<sub>3</sub>CN and 1 mL of pyridine. The solution, stirred in nitrogen atmosphere, was taken at reflux temperature and then, five drops of piperidine were added. The solution was refluxed overnight and then cooled down to room temperature. The precipitation of a compound occurred, that was then recovered by filtration and recrystallized by THF-hexane. An amorphous blue solid was obtained. Yield was 65 %.

<sup>1</sup>H-NMR (DMSO, 500 MHz): δ= 0.76 (t, 6H, J=7.0 Hz, -CH<sub>3</sub>); 0.85 (t, 6H, J=7.0 Hz, -CH<sub>3</sub>); 1.16-1.32 (m, 16H, -CH<sub>2</sub>); 1.97 (m, 2H,-CH); 4.29 (d, 4H, J=6.0 Hz, N-CH<sub>2</sub>); 6.53 (d, 2H, J=15.0 Hz, CH=CH); 7.11 (s, 2H, Ar-H); 7.41 (d, 2H, J=10.5 Hz, Ar-H); 7.54 (d, 2H, J=8.0 Hz, Ar-CH); 7.62 (d, 2H, J=8.0 Hz, Ar-H); 7.74 (d, 2H, J=15.0 Hz, CH=CH); 7.78-7.83 (m, 4H, Ar-H); 7.96 (d, 2H, J=8.0 Hz, Ar-H); 8.04-8.07 (m, 3H, Ar-H); 8.48 (s, 2H, Ar- H); 8.53 (d, 1H, J=7.5 Hz, Ar-H); 8.67 (s, 2H, Ar-H); 12.17 (s broad, 2H).

<sup>13</sup>C-NMR (DMSO, 75 MHz): δ= 172.2; 167.9; 161.3; 145.3; 144.9; 142.4; 142.0; 140.6; 137.9; 134.0; 126.5; 126.0; 122.7; 122.5; 121.4; 121.1; 121.0; 117.2; 116.3; 116.0; 111.0; 110.3; 59.0; 46.8; 30.1; 28.0; 23.6; 22.5; 13.8; 10.6.

MALDI-TOF-MS: Found: 1054.78; 'Molecular formula C<sub>67</sub>H<sub>62</sub>N<sub>4</sub>O<sub>6</sub> requires': 1054.43.

CHN elemental analysis: Found: C 75.34 H 5.85 N 5.19 %; 'Molecular Formula C<sub>66</sub>H<sub>62</sub>N<sub>4</sub>O<sub>7</sub>S requires': C 75.12; H 5.92; N 5.31; O 10.61; S 3.04 %.

## 2.2. Chemical Physical characterization

All compounds were characterized by standard techniques. <sup>1</sup>H NMR Spectra were recorded with Varian XL 200, Bruker 400 or Varian 500 MHz spectrometers. DSC analyses were performed in dry ultrapure nitrogen flow using a DSC7 PerkinElmer apparatus at a scan rate of 10 K/min; DSC temperature calibration was made using a Perkin Elmer indium sample having 99.999% purity.

Solution and thin film UV-Vis spectra were recorded on a spectrophotometer Jasco V-560 (scan rate 200 nm min<sup>-1</sup>). Thin film of chromophores were prepared by spin coating of a DMF solution (10 mg·mL<sup>-1</sup>) on glass substrates, using a Laurell WS-650Mz-23NPP spin processor .

### 2.3. Electrochemical characterization

Electrochemical measurements were performed with a Metrohm 757 VA Computrace combined with a AUTOLAB potentiostat-galvanostat. Voltammetric experiments were run under nitrogen on thin films of the chromophores deposited on the working electrode, at a 100 mV/sec scan speed and at room temperature, ranging between 0÷1.5 V. A single compartment three-electrode cell have been employed, with a glassy carbon working electrode, using Ferrocene/Ferrocinium (Fc/Fc<sup>+</sup>) redox couple as internal reference as suggested by IUPAC for organic systems. Tetrabutylammonium hexafluorophosphate (100 mM) served as inert electrolyte.

### 2.4. Computational analysis

The electronic structures of the ground and the excited states were determined at density functional theory (DFT) level, using the CAM-B3LYP functional and the 6-31+G(d,p) basis set. CAM-B3LYP was chosen as it holds a high percentage of Hartree-Fock exchange, which is known to give more accurate results than standard hybrid functionals for donor-acceptor conjugate dyes.<sup>20a-c</sup> Solvent effects, dimethylformamide, have been included by using the Polarizable Continuum Model (PCM).<sup>20d</sup> All the alkyl substituents have been replaced by methyl groups. Conformational analyses have been performed by using the Spartan package and the Merck molecular force field.<sup>19e</sup> All computations have been performed by G09 package.<sup>20f</sup>

### 2.5. DSSC materials, assembly and measurement system

Titania pastes 18NR-T (transparent  $\phi \approx 21\text{nm}$ ) and 18NR-AO (opaque  $\phi \approx 20\text{-}300\text{nm}$ ) Dyesol were used as received and screen printed on glass substrates (Pilkington). After relaxation the substrates were sintered at 525 °C for 30 minutes. Counterelectrodes were made by screen printing the platinum paste (Kimet) and fired at 425°C for 20 minutes. The sintered TiO<sub>2</sub> were immersed in the different tetrahydrofuran solution of dyes overnight (10<sup>-4</sup> M, 14-16 hours) at room temperature. Substrates then have been rinsed with

tetrahydrofuran and dried. Surlyn 25 Solaronix is used to seal the photo and counter-electrodes and the High Stability Electrolyte Dyesol is introduced within the electrodes.

Measurements have been carried out by means of a solar simulator ABET 2000 sun simulator supplied with a filter AM1.5 under illumination at  $0.1\text{W}/\text{cm}^2$ .

### 3. Results and discussion

#### 3.1. Synthesis

Commercial 2,6-dimethyl- $\gamma$ -pyrone is the starting compound in the synthesis of all the reported chromophores. Its ketone group can be easily functionalized by means of a condensation reaction with compounds containing an acidic methylene group. In Scheme 2, the synthesis of four different derivatives, representing the acceptor core of the designed chromophores, is reported; the reaction was performed in acetic anhydride and the pyrone molecule was reacted with groups featuring different electron-withdrawing (EWD) strength.

The synthesis of the donor branches of the dyes is schematically shown in Scheme 3. The key reaction is the Heck coupling between the bromo-formyl derivative of carbazole (3) and acrylic acid.

The obtained compound contains a formyl group that can react with the methyl groups of the acceptor cores ( $A_n$ ) in a Knoevenagel type condensation, affording the desired dyes (see Scheme 3).

All the prepared chromophores show good solubility in solvent like THF and DMF. They show a poor tendency to crystallize and were generally recovered as amorphous powders. In one case, namely for  $C_1$ , DSC analysis makes it possible to measure the glass transition temperature ( $T_g = 210\text{ }^\circ\text{C}$ ).

#### 3.2. Optical and electrochemical analysis

The optical properties of the dyes were investigated by UV-Vis analysis performed in DMF solution. The strength of the EWD group functionalizing the pyran core has a marked effect on the absorption spectrum of the chromophores: in particular, the stronger is the electron acceptor group, the more red-shifted is the absorption spectrum (see Figure 1). A set of colors ranging from orange to blue is obtained that covers a large part of the visible spectrum. All the chromophores show very high molar absorption coefficient, ranging from  $6 \cdot 10^4$  to  $1 \cdot 10^5 \text{ L} \cdot \text{mol}^{-1} \cdot \text{cm}^{-1}$ , a highly desirable feature for their application as photosensitizers in DSSC.

Because of the low tendency to crystallize, it was possible to prepare amorphous thin films of the chromophores by spin coating from DMF solution. The UV-Vis absorption spectra of the films are shown in Figure 2: for all the chromophores but  $C_3$ , a slight bathochromic shift of the absorption features is observed as compared to their behaviour in DMF solution. The optical bandgap of chromophores in thin films was measured by applying the Tauc extrapolation to the absorption spectra,<sup>21</sup> and range from 2.24 eV ( $C_1$ ) to 1.65 eV ( $C_4$ ). The optical properties of the dyes are summarized in Table 1.

The photoluminescence properties of the dyes were investigated in THF solution.  $C_1$  and  $C_2$  show a photoluminescence quantum yield of, respectively, 2.1 and 0.7 %. The values were calculated using quinine sulfate as fluorescence standard. Dyes  $C_3$  and  $C_4$  feature no fluorescence at all. The fluorescence spectra of chromophores  $C_1$  and  $C_2$  are reported as supplementary data (Figure S2).

Oxidation potentials of the chromophores have been measured by means of cyclic voltammetry (Figure 3), using the redox couple ferrocene/ferrocinium ( $\text{Fc}/\text{Fc}^+$ ) as internal standard. From the voltammograms, shown in Figure 3, chromophore's HOMO energies have been determined by applying the formula:

$$E_{HOMO} = -(E_{onset,ox} - E_{Fc/Fc^+} + 5.1)$$

The HOMO energy slightly differs for each chromophores: except for  $C_2$ , the observed trend seems to suggest that, by increasing the strength of the EWD group functionalizing the pyran core, the HOMO energy of the dye is stabilized. All the measured values are much lower than the oxidation potential of the redox

couple  $I/I^{3-}$  (-4.8 eV), generally used in DSSC devices, so that sensitizer regeneration during DSSC operation should not pose problems.

LUMO energies of dyes have been obtained from the optical bandgaps, by applying:

$$E_{LUMO} = E_{HOMO} + E_g$$

LUMO energies of the dyes are reported in Table 1: during DSSC operation, electron injection from the excited state of the dye to the conduction band of  $TiO_2$  has a driving force related to the energy difference between dye's LUMO and the edge of  $TiO_2$  conduction band ( $E_{CB}$ ). The commonly accepted values for the latter, in DSSC literature, range from -4.25 to 3.95 eV.<sup>22</sup> As observed from Figure 4, this band alignment requirement is satisfied for chromophores  $C_1$  and  $C_2$ , while dyes  $C_3$  and  $C_4$  have LUMO energies very close to the  $E_{CB}$  of  $TiO_2$ , so that the electron injection process from the chromophore to the oxide could be less efficient.

### 3.3. Computational Analysis

To gain information about the electronic structures of the ground and the excited states of the four dyes we have carried out a computational analysis at density functional theory (DFT) level. DFT computations were preceded by a full conformational analysis, focusing attention on the geometrical arrangements of the carbazolic branches with respect to the pyranic core. The lowest energy conformations of all the chromophores in the gas phase exhibit a s-trans arrangement of the conjugated C=C bonds of the pyran ring and the ethylene bridge connecting it to the carbazole moieties. Indeed the s-trans conformation allows, in the gas-phase, the formation of a strong intramolecular hydrogen bond between the two carbazolic branches. Apart from that, molecular mechanics computations predict that the s-trans conformation is more stable than the s-cis one by ca. 1.6 kcal/mol, for each C=C double bond, and it will be therefore retained even when the intramolecular H-bonds are disrupted. We have thus started all electronic computations from trans conformations of both carbazolic branches.

The results of DFT computations are summarized in Table 2, where the predicted absorption wavelengths and oscillator strengths have been reported, together with the dipole moments of the ground states and of the first excited singlets.

Chromophores **C<sub>1</sub>** and **C<sub>2</sub>** can be classified as standard push-pull molecules inasmuch as the dipole moments of the first excited state are significantly larger than the ground state ones. Indeed, computations predict that excitation to the first excited singlet causes a transfer of electron density from the carbazolic moieties towards the acceptor core, as shown in Figure 5, where the electron density changes upon transition to the first excited state are reported for all the chromophores.

Chromophores **C<sub>3</sub>** and **C<sub>4</sub>** behave differently, their ground state dipole moments do not significantly increase upon excitation, see Table 2, and the electronic transitions are no longer charge transfer transitions; Figure 5 in fact shows that in the case of **C<sub>3</sub>**, and **C<sub>4</sub>** electron density changes upon transition to the first excited singlet are localized on the pyranic core and on the EWD group. Analysis of the electronic distribution in the ground electronic state show that the net charge on the EWD group significantly increases for **C<sub>3</sub>** and **C<sub>4</sub>** with respect to **C<sub>1</sub>** and **C<sub>2</sub>**, being approximately -1 for **C<sub>4</sub>**, the strongest EWD group. Thus by increasing the strength of the EWD group functionalizing the pyran core, the electronic structures of the chromophores can be finely tuned from that well characteristic of a push-pull dye toward zwitterionic structures.<sup>23</sup>

In Table 2 the predicted vertical absorption wavelengths are reported. Since the synthesized dyes consist of symmetric heterotrimers, two transitions in the same spectral region occur because of exciton coupling.<sup>24</sup> The observed shifts at longer wavelengths, about 100 nm for each heterotrimer with respect to the absorption wavelength of the individual components, has to be attributed either to the CT character of the transitions, especially for **C<sub>1</sub>** and **C<sub>2</sub>**, or to electronic interactions between the carbazolic and the pyranic core in the ground state.

The computed oxidation potentials are reported in Table 2. All dyes are characterized by high oxidation potentials, larger than carbazole one, because of the presence of strong electron acceptor groups. As

shown in figure 6, the electron hole of the oxidized species mainly resides on the carbazolic branches for all the four chromophores.

### 3.4. Photovoltaic measurements

All the synthesized chromophores were used as TiO<sub>2</sub> sensitizers in standard DSSCs (0.25 cm<sup>2</sup>). Two kinds of photoanode were used to which we will refer as transparent titania, in which the average nanoparticle diameter is 21 nm, and opaque titania, which is constituted by a mixture of nanoparticles of different size, ranging from 20 to 350 nm. The redox couple used was I<sup>-</sup>/I<sub>3</sub><sup>-</sup>. Details about cell fabrication are reported in the Experimental Section.

J/V curves, recorded under AM1.5 G simulated solar irradiation (at incident power of 100 mW/cm<sup>2</sup>) are reported in Figure 6, while the main electrical parameters of the fabricated cells, are summarized in Table 3.

DSSC efficiencies are related both to the dye and to the type of photoanode used: as far as the latter is concerned, better results are obtained using the opaque titania. This is related to light trapping effect occurring with this kind of photoanode, because of the incoherent light reflection inside the DSSC, that results in an increased photon absorption and hence, an increased charge photogeneration.

Regarding the dyes, the best results are obtained with the sensitizers **C<sub>1</sub>** and **C<sub>2</sub>**, which afford power moderate conversion efficiency up to, respectively, 1.90 % and 1.70 %, notwithstanding the low electron density around the carboxylic groups (anchoring points to the oxide) highlighted by DFT calculations: the peculiar conformation adopted by the chromophores, emerged by DFT analysis, suggests an anchoring mode on TiO<sub>2</sub> in which the two carboxylic simultaneously link to the metal, allowing the electron rich area of chromophore's LUMO to approach the oxide surface, thus favouring the electron injection process.

The electrical parameters are characterized by the fact that the open circuit voltage (V<sub>oc</sub>) remains quite low (600mV and less), affecting the PCE of the cells, and this is due to multiple reasons. It is known that the

maximum photovoltage ( $V_{\max}$ ) obtained in the DSSC is attributed to the energy gap between the quasi-Fermi level (approximately the energy level of the conduction-band edge) of the  $\text{TiO}_2$  and the redox potential of the electrolyte. Moreover it is crucial to have complete titania covering by the dye in order to avoid undesirable recombination, hence voltage drop, between the generated charge injected into the  $\text{TiO}_2$  network and the electrolyte solution.<sup>25</sup> To this end the dye must be tailored to efficiently bond to the  $\text{TiO}_2$ , having minimal distance between adjacent molecules, minimum steric hindrance between them and so less  $\text{TiO}_2$ -electrolyte interface. In the present case it seems that the dye covering of the titania should be enhanced and this can be done by using a proper solvent,<sup>26</sup> change the type of titania paste, i.e. porosity, grain size, hence the dye coverage,<sup>27</sup>  $\text{TiCl}_4$  treatment<sup>28</sup> and so on. In the present study, we meant to investigate the effectiveness of the novel synthesized photosensitizers in standard conditions, reserving the possibility of optimize their performance in further studies. Indeed, despite the low voltage, there is charge injection, hence a certain  $J_{\text{sc}}$  and this is due to the correct alignment of the HOMO level with respect to the  $\text{TiO}_2$ -CB, demonstrating the efficacy of the, at least,  $\text{C}_1$  and  $\text{C}_2$ . For what concerns  $\text{C}_3$  and  $\text{C}_4$ , these dyes give rise to devices with poor efficiency. As previously anticipated, this can be related with a poor driving force in the process of electron injection from the excited state of the chromophore (see Figure 4). It is known from the literature that a poor efficiency in the electron injection process results in a diminished photocurrent (low  $J_{\text{sc}}$ ) and also negatively affects the cell  $V_{\text{oc}}$  and FF, thus strongly limiting the PCE. The less efficient photosensitizer is hence  $\text{C}_4$ , which features a LUMO energy even lower than the conduction band edge of  $\text{TiO}_2$ .

#### 4. Conclusions

We have reported the synthesis and characterization of four novel chromophores characterized by a donor-acceptor-donor molecular structure and based on a pyran core symmetrically linked to two carbazole donor moieties. All chromophores feature high extinction coefficients, up to  $1.0 \cdot 10^5 \text{ L} \cdot \text{mol}^{-1} \cdot \text{cm}^{-1}$ . By functionalizing the pyran core with groups characterized by different electron withdrawing (EWD) activity,

it was possible to tune the optical properties of the resulting dyes: in particular, the higher is the EWD strength of the substituents, the more red shifted is the chromophore absorption. A set of colors ranging from orange to blue was obtained, so that most of the visible spectrum was covered. Cyclic voltammetry studies performed on the dyes in combination with optical measurement, gave some indication about the energy of their frontier molecular orbitals: from this combined analysis, it came out that the LUMO energy is deeply influenced by the EWD power of the group functionalizing the pyran core of the chromophores. Chromophores  $C_3$  and  $C_4$ , in particular, show very high electron affinity, with LUMO energies close to the commonly reported value for  $E_{CB}$  of titanium dioxide. The electronic properties of the dyes were investigated at DFT level: for all the chromophores the electron density around the carboxylic groups is depleted upon excitation and mainly shifted on the pyran core, so that the process of electron injection in  $TiO_2$  conducting band could be negatively affected.

The chromophores were investigated as photosensitizers in DSSC: as expected, the performances of devices based on  $C_3$  and  $C_4$  are rather low: the reason for low efficiency derived from the high electron affinity of the dyes that negatively influenced the process of electron transfer in the conduction band of titania. A moderate efficiency, close to 2 % was instead obtained for devices based on  $C_1$  and  $C_2$ , notwithstanding the low electron density around the carboxylic groups (anchoring points to the oxide) highlighted by DFT calculations: we speculated on the possibility that, the conformation adopted by the chromophores, suggested by DFT analysis, could result in a specific anchoring arrangement that might help the electron transfer by placing the electron rich pyran core in the proximity of the oxide surface.

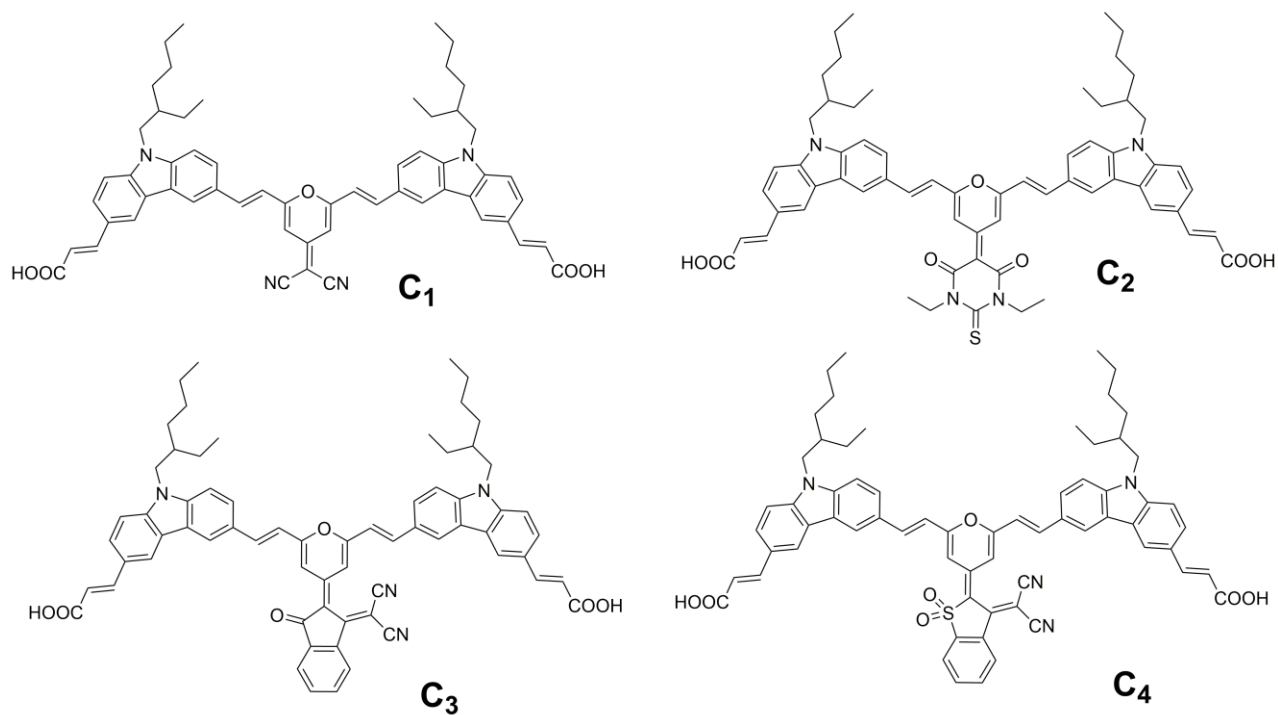
## References

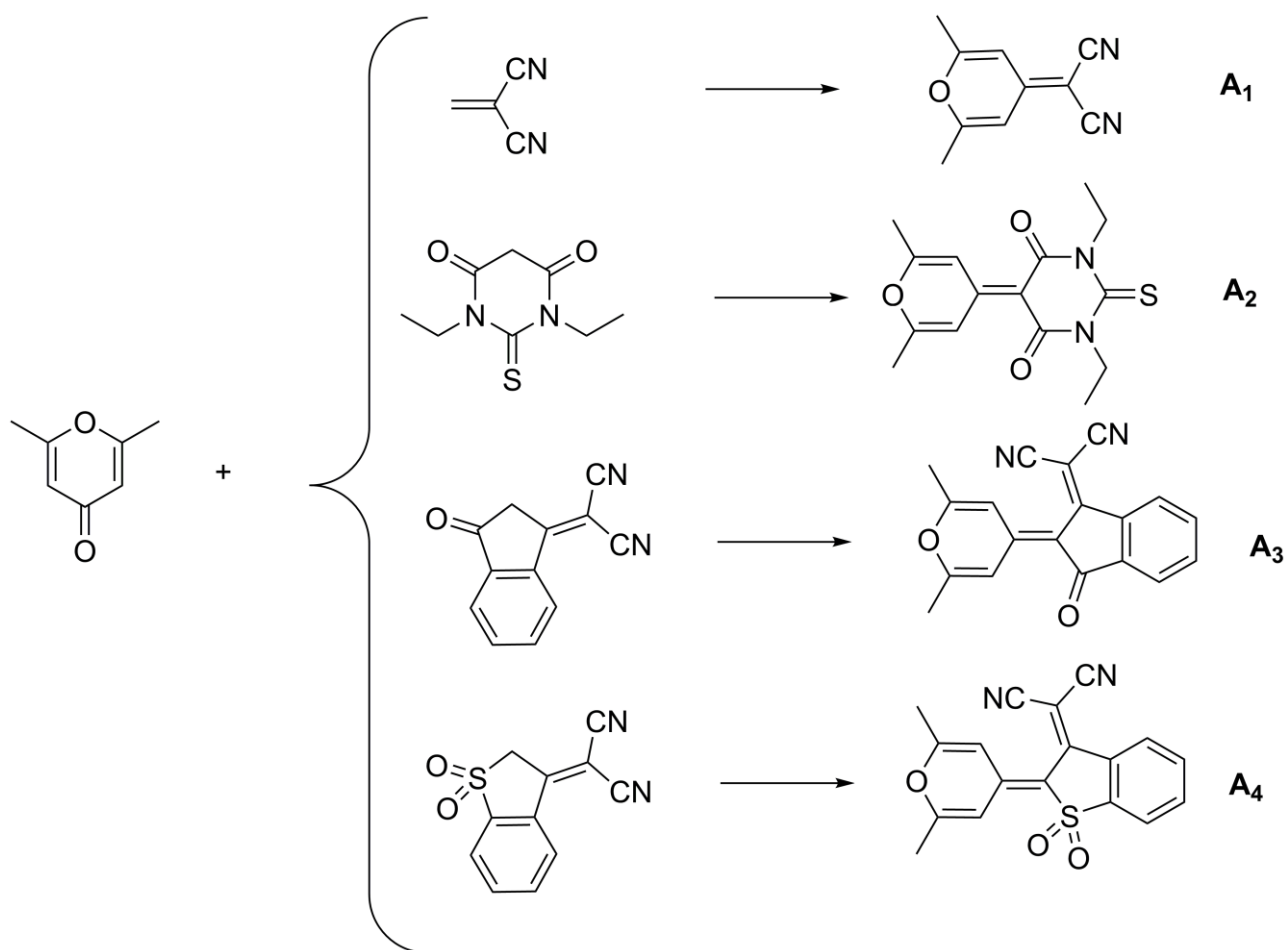
- 1) N. S. Lewis, D. G. Nocera, *P.Natl. Acad. Sci. USA*, **2006**, *103*, 15729-15735.
- 2) a) A. Hegfeldt, G. Boschloo, L. Sun, L. Kloo, H. Pettersson, *Chem. Rev.*, **2010**, *110*, 6595-6663; b) J. Gong, J. Liang, K. Sumathy, *Renewable and Sustainable Energy Reviews*, **2012**, *16*, 5848-5860; c) M. K. Nazeeruddin, E. Baranoff, M. Grätzel, *Solar Energy*, **2011**, *85*, 1172-1178; d) A. B. F. Martinson, T. W. Hamaann, M. J. Pellin, J. T. Hupp, *Chem. Eur. J.*, **2008**, *14*, 4458-4467; e) M. Grätzel, *Inorg. Chem.*, **2005**, *44*, 6841-6851.
- 3) a) Y. Chiba, A. Islam, Y. Watanabe, R. Komiya, N. Koide, L. Han, *Jpn. J. Appl. Phys.*, **2006**, *45*, L638-L640; b) M. K. Nazeeruddin, F. De Angelis, S. Fantacci, A. Selloni, G. Viscardi, P. Liska, S. Ito, B. Takeru, M. Grätzel, *J. Am. Chem. Soc.*, **2005**, *127*, 16835-16847.
- 4) a) A. Mishra, M. K. R. Fisher, P. Bauerle, *Angew. Chem. Int. Ed.*, **2009**, *48*, 2474-2499; b) R. K. Kanaparthi, J. Kandhadi, L. G. Giribabu, *Tetrahedron*, **2012**, *68*, 8383-8393; c) D. Franchi, M. Calamante, G. Reginato, L. Zani, M. Peruzzini, M. Taddei, F. Fabrizi de Biani, R. Basosi, A. Sinicropi, D. Colonna, A. Di Carlo, A. Mordini, *Tetrahedron*, **2014**, *70*, 6285-6295.
- 5) (a) U. Caruso, R. Centore, A. Roviello, A. Sirigu, *Macromolecules*, **1992**, *25*, 2290-2293; (b) R. Centore, B. Panunzi, A. Roviello, A. Sirigu, P. Villano, *J. Polym. Sci. Part A Polym. Chem.*, **1996**, *34*, 3203-3211.
- 6) (a) R. Centore, S. Concilio, B. Panunzi, A. Sirigu, N. Tirelli, *J. Polym. Sci. Part A Polym. Chem.*, **1999**, *37*, 603-608; (b) A. Carella, R. Centore, P. Riccio, A. Sirigu, A. Quatela, C. Palazzesi, M. Casalbani, *Macromol. Chem. Phys.*, **2005**, *206*, 1399-1404; (c) S. Fusco, R. Centore, P. Riccio, A. Quatela, G. Stracci, G. Archetti, H.-G. Kuball, *Polymer* **2008**, *49*, 186-191; d) F. Borbone, A. Carella, L. Ricciotti, A. Tuzi, A. Roviello, A. Barsella, *Dyes and Pigments*, **2011**, *88*, 290-295.
- 7) (a) A. Pron, P. Gawrys, M. Zagorska, D. Djurado, R. Demadrille, *Chem. Soc. Rev.*, **2010**, *39*, 2577-2632; (b) W. H. Lee, J. Park, S. H. Sim, S. Lim, K. S. Kim, B. H. Hong, K. Cho, *J. Am. Chem. Soc.*, **2011**, *133*, 4447-4454; (c) R. Centore, L. Ricciotti, A. Carella, A. Roviello, M. Causà, M. Barra, F. Ciccullo, A.

- Cassinese, *Org. Electr.*, **2012**, *13*, 2083-2093; d) A. Carella, F. Borbone, A. Roviello, G. Roviello, A. Tuzi, A. Kravinsky, R. Shikler, G. Cantele, D. Ninno, *Dyes and Pigments*, **2012**, *95*, 116-125.
- 8) a) R. Centore, C. Manfredi, S. Fusco, C. Maglione, A. Carella, A. Capobianco, A. Peluso, D. Colonna, A. Di Carlo, *J. Mol. Struct.*, **2015**, *1093*, 119-124; b) L. Zhang, J. M. Cole, *ACS Appl. Mat. Interfaces*, **2015**, *7*, 3427-3455.
- 9) a) T.H. Liu, C.Y. Lou, C. H. Chen, *Appl. Phys. Lett.*, **2003**, *83*, 5241-5243; b) K. H. Lee, Y. K. Kim, S. S. Yoon, *Bull. Kor. Chem. Soc.*, **2012**, *33*, 3433-3436.
- 10) A. Carella, F. Borbone, U. Caruso, R. Centore, A. Roviello, A. Barsella, A. Quatela, *Macromol. Chem. Phys.*, **2007**, *208*, 1900-1907.
- 11) a) A. Ambrosio, E. Orabona, P. Maddalena, A. Composeo, M. Polo, A. A. R. Neves, D. Pisignano, A. Carella, F. Borbone, A. Roviello, *Appl. Phys. Lett.*, **2009**, *94*, 011115; b) A. Ambrosio, P. Maddalena, A. Carella, F. Borbone, A. Roviello, M. Polo, A. A. R. Neves, A. Composeo, D. Pisignano, *J. Phys. Chem. C*, **2011**, *28*, 13566-13570.
- 12) L. Xue, Y. Li, F. Dong, W. Tian, *Nanotechnology*, **2010**, *21*, 155201 (pp. 1-10).
- 13) a) S. Franco, J. Garin, N. Martinez de Boroja, R. Perez-Tejada, J. Orduna, Y. Yu, M. Lira-Cantù, *Org. Lett.*, **2012**, *14*, 752-755; b) J. G. Awuah, J. Polreis, J. Prakash, Q. Qiao, Y. You, *J. Photochem. Photobiol. A: Chem*, **2011**, *224*, 116-122.
- 14) a) R. Misra, T. Jadhav, B. Dhokale, P. Gautam, R. Sharma, R. Maragani, S. M. Mobin, *Dalton Trans.*, **2014**, *43*, 13076-13086; b) T. Jadhav, R. Misra, S. Biswas, G. D. Sharma, *Phys. Chem. Chem. Phys.*, **2015**, *17*, 26580-26588.
- 15) a) S. Pramjit, V. Eiamprasert, P. Surawatanawong, P. Lertturongchai, S. Kiatisevi, *J. Photochem. Photobiol. A: Chemistry*, **2015**, *296*, 1-10; b) A. El Shaffei, M. Hustain, A. Atiq, A. Islam, L. Han, *J. Mater. Chem.*, **2012**, *22*, 24048-24056; c) A. Venkateswararao, K. R. J. Thomas, C. P. Li, C. T. Lee, K. C. Ho, *ACS Appl. Mat. Interf.*, **2014**, *6*, 2528-2539.
- 16) a) R. Sirohi, D. H. Kim, S. C. Yu, S. H. Lee, *Dyes and Pigments*, **2012**, *92*, 1132-1137; b) G. Wu, F. Kong, Y. Zhang, J. Li, W. Chen, C. Zhang, S. Dai, *Dyes and Pigments*, **2014**, *105*, 1-6; c) A. Abboto, N.

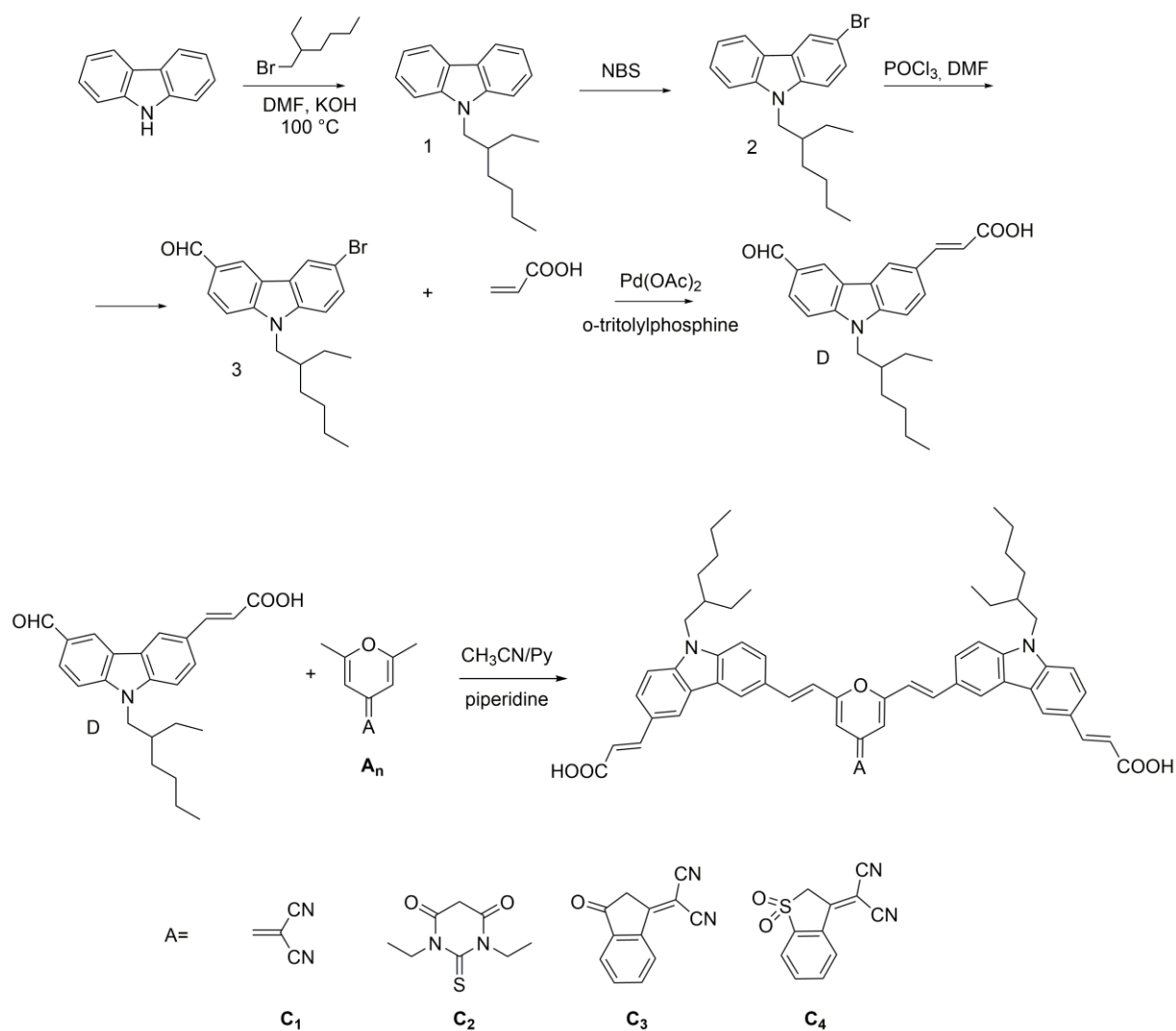
- Manfredi, C. Marini, F. De Angelis, E. Mosconi, J.-H. Yum, Z. Xianxi, M. K. Nazeeruddin, M. Grätzel, *Energy Environ. Sci.*, **2009**, *2*, 1094-1101; d) D. Heredia, J. Natera, M. Gervaldo, L. Otero, F. Fungo, C.-Y. Lin, K.-T. Wong, *Org. Lett.*, **2010**, *12*, 12-15.
- 17) a) P. Gautam, R. Maregani, R. Misra, *Tetrahedron Lett.*, **2014**, *55*, 6827-6830; b) R. Misra, P. Gautam, S. M. Mobin, *J. Org. Chem.*, **2013**, *78*, 12440-12452.
- 18) K. Bello, L. Cheng, J. Griffiths, *J. Chem. Soc. Perkin. Trans. II*, **1987**, 815-818.
- 19) W. Baumann, **1979**, *UK Patent* 2026528.
- 20) a) A. Capobianco, R. Centore, C. Noce, A. Peluso, *Chem. Phys.*, **2013**, *411*, 11-16; b) A. Capobianco, R. Centore, S. Fusco, A. Peluso, *Chem. Phys. Lett.*, **2013**, *580*, 126-129; c) R. Centore, S. Fusco, A. Capobianco, V. Piccialli, S. Zaccaria, A. Peluso, *Eur. J. Org. Chem.*, **2013**, 3721-3728; d) S. Miertus, E. Scrocco, J. Tomasi, *Chem. Phys.*, **1981**, *55*, 117-129; e) Spartan'04, Wavefunctions Inc., Irvine. CA; f) M. J. Frisch *et al*, Gaussian 09, Revision **D.01**, Gaussian, Inc., Wallingford CT, 2009.
- 21) J. Tauc, R. Grigorovici, A. Vancu, *Phys. Status Solidi B*, **1966**, *15*, 627-637.
- 22) a) M. Grätzel, *Nature*, **2001**, *414*, 338-344; b) I. Chung, B. Lee, J. He, R. P. H. Chang, M. G. Kanatzidis, *Nature*, **2012**, *485*, 486-489; c) M. Liang, J. Chen, *Chem. Soc. Rev.*, **2013**, *42*, 3453-3488.
- 23) a) A. Capobianco, A. Esposito, T. Caruso, F. Borbone, A. Carella, R. Centore, A. Peluso, *Eur. J. Org. Chem.*, **2012**, 2980-2989; b) P. A. Bouit, C. Aronica, L. Toupet, B. Le Guennic, C. Andraud, O. Maury, *J. Am. Chem. Soc.* **2010**, *132*, 4328-4335.
- 24) C. Lambert, T. Scherpf, H. Ceymann, A. Schmediel, M. Holzapfel, *J. Am. Chem. Soc.*, **2015**, *137*, 3547-3557.
- 25) K. Kakiage, Y. Aoyama, T. Yano, T. Otsuka, T. Kyomen, M. Unno, M. Hanaya, *Chem. Commun.*, **2014**, 6379-6381.
- 26) H. Ozawa, M. Awa, T. Ono, H. Arakawa, *Chem. Asian. J.*, **2012**, *7*, 156-162.
- 27) T. P. Chou, Q. Zhang, B. Russo, G. E. Fryxell, G. Cao, *J. Phys. Chem. C.*, **2007**, *111*, 6296-6302.
- 28) L. Vesce, R. Riccitelli, G. Soscia, T. M. Brown, A. Di Carlo, A. Reale, *J. Non-Cryst. Solids*, **2010**, *356*, 1958-1961.

Figure Captions

**Scheme 1.** Molecular structure of the synthesized dyes.



**Scheme 2.** Functionalization of the pyran core with different electron withdrawing groups



**Scheme 3.** Synthesis of the electron donor carbazolic branches and of the final chromophores

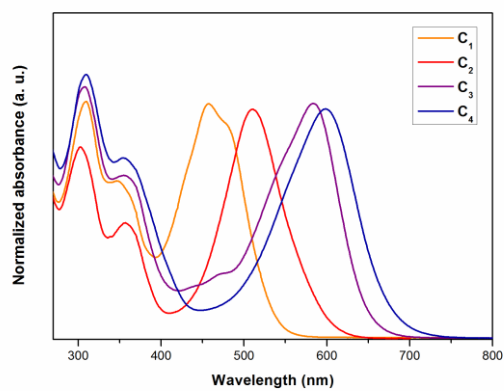


**Figure 1.** Normalized absorption spectra of the synthesized chromophores in DMF

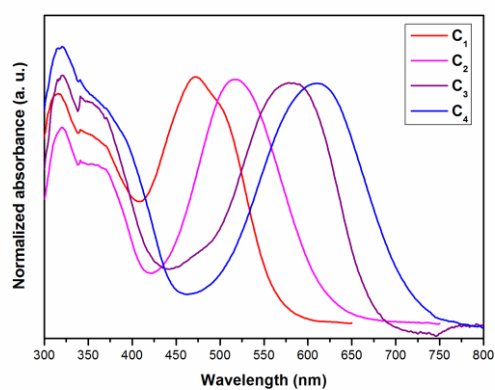


**Figure 2.** Normalized absorption spectra of the synthesized chromophores as thin films spin coated on glass substrates.

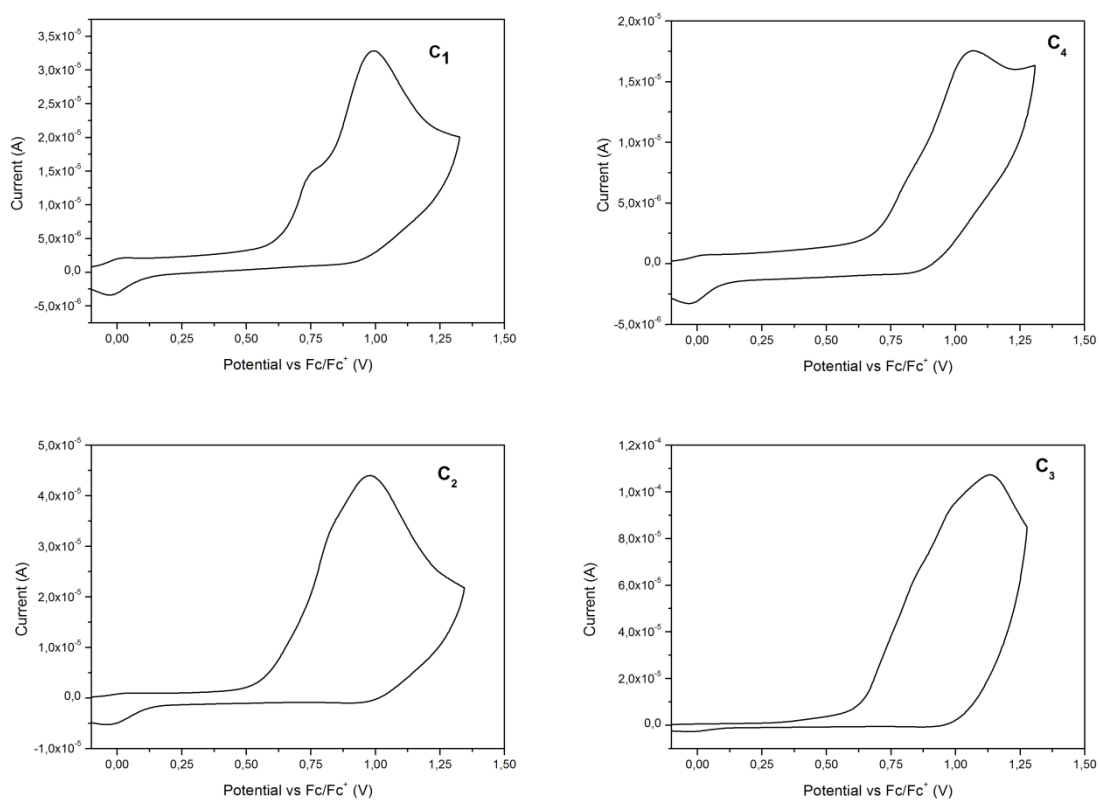


**Figure 3.** Voltammograms of the prepared dyes.

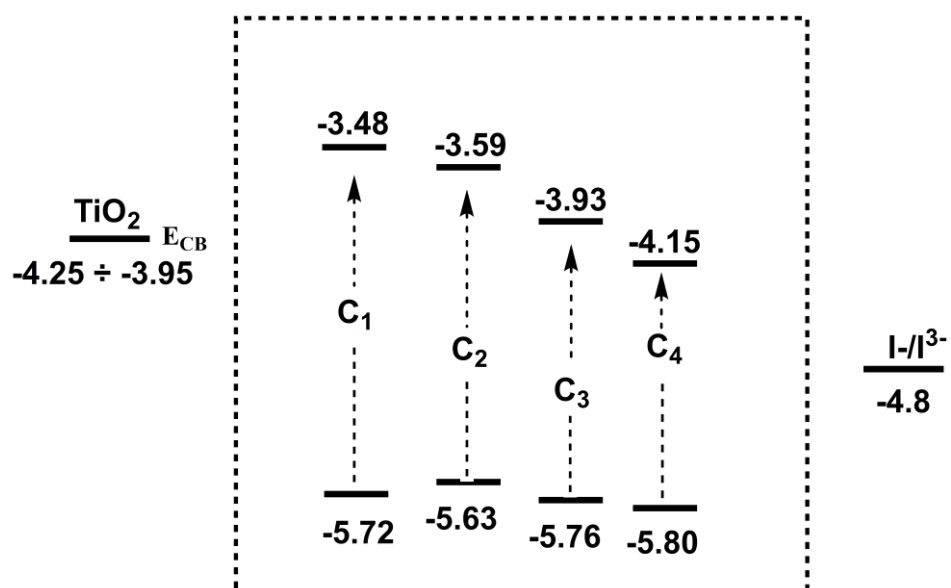
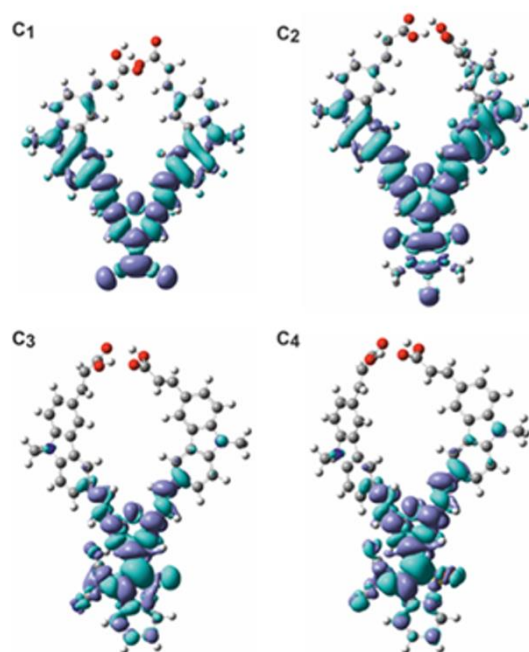
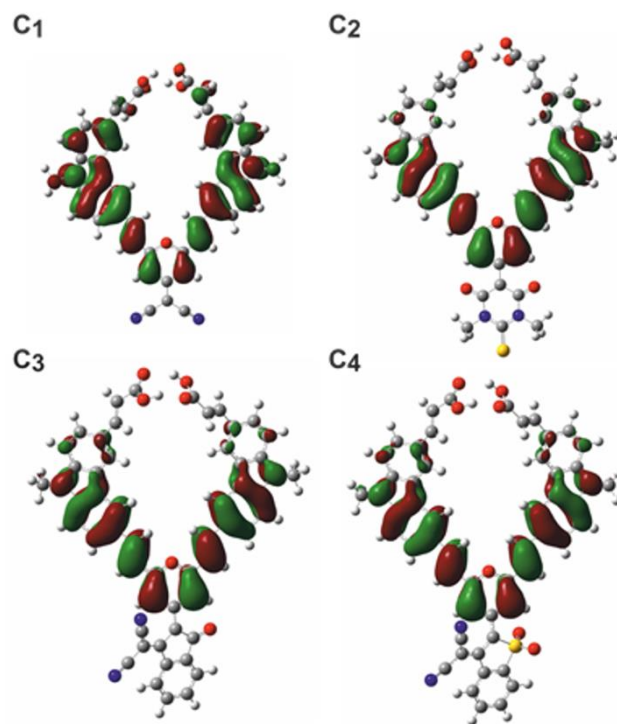


Figure 4. Band alignment of the synthesized dyes with the conduction band of  $\text{TiO}_2$  and the oxidation potential of the redox couple  $\text{I}^-/\text{I}_3^-$ .



**Figure 5.** Computed electronic density variation upon excitation to the first excited singlet of  $C_1$ - $C_4$ . The violet and blue lobes represent electron density increase and depletion upon excitation, respectively



**Figure 6.** *Computed isodensity surfaces of LUMO of cationic dyes*

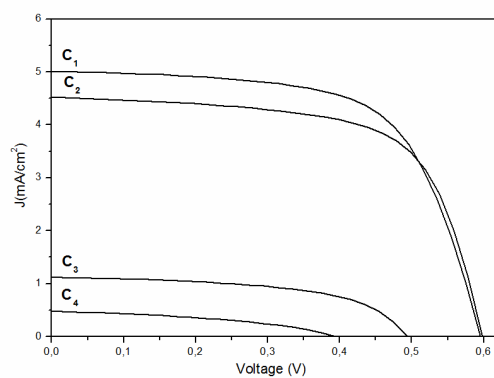


**Figure 7.** Representative  $J/V$  curves for the fabricated DSSC containing the synthesized dyes

Tables

**Table 1.** Optical and electrochemical properties of the synthesized chromophores

Dye	$\lambda_{\max}$ (nm) <sup>a</sup>	$\lambda_{\max}^{\text{film}}$ (nm) <sup>b</sup>	$\epsilon$ (L·mol <sup>-1</sup> ·cm <sup>-1</sup> ) <sup>a</sup>	$E_g$ (eV) <sup>c</sup>	$E_{\text{onset,ox vs Fc/Fc}^+}$ (V)	HOMO (eV)	LUMO (eV)
C <sub>1</sub>	457	472	$1,0 \cdot 10^5$	2.24	0.62	-5,72	-3,48
C <sub>2</sub>	510	518	$9,4 \cdot 10^4$	2.04	0.53	-5,63	-3,59
C <sub>3</sub>	583	581	$8,4 \cdot 10^4$	1.83	0.66	-5,76	-3,93
C <sub>4</sub>	598	610	$6,5 \cdot 10^4$	1.65	0.70	-5,80	-4,15

*a) Scan rate 200 nm/min, in DMF solution; b) thin film spin coated from DMF solution; c) determined from absorption spectra of the film by applying the Tauc relationship (ref.21)*

**Table 2.** Electronic properties of the synthesized chromophores, computed at DFT level.

	$\mu_0$ (Debye)	$\mu_{ex}$ (Debye)	$P_{ox}$ (eV)	$\lambda_{theo}$ (nm)	F
<b>C<sub>1</sub></b>	12.53	23.25	5.70	426.72	0.57
				404.89	3.11
<b>C<sub>2</sub></b>	12.92	24.14	5.85	458.66	0.67
				425.00	2.67
<b>C<sub>3</sub></b>	14.23	15.01	5.88	493.77	1.62
				467.21	0.60
<b>C<sub>4</sub></b>	13.79	13.86	5.91	506.84	1.64
				492.24	0.60

**Table 3.** Electrical parameters of the fabricated DSSC

Dye	TRANSPARENT TITANIA				OPAQUE TITANIA			
	$V_{oc}$ (mV)	$J_{sc}$ (mA/cm <sup>2</sup> )	FF(%)	$\eta$ (%)	$V_{oc}$ (mV)	$J_{sc}$ (mA/cm <sup>2</sup> )	FF(%)	$\eta$ (%)
<b>C<sub>1</sub></b>	605	4.25	70	1.80	595	5.00	64	1.90
<b>C<sub>2</sub></b>	600	3.85	70	1.60	595	4.35	65	1.70
<b>C<sub>3</sub></b>	500	0.85	61	0.26	490	1.10	55	0.30
<b>C<sub>4</sub></b>	410	0.27	47	0.05	395	0.43	42	0.07